The Astrophysical Journal, 676:1151–1161, 2008 April 1

SPATIALLY RESOLVED PROPERTIES OF THE GRB 060505 HOST: IMPLICATIONS FOR THE NATURE OF THE PROGENITOR[1]

Christina C. Thöne,[2] Johan P. U. Fynbo,[2] Göran Östlin,[3] Bo Milvang-Jensen,[2] Klaas Wiersema,[4] Daniele Malesani,[2] Desiree Della Monica Ferreira,[2] Javier Gorosabel,[5] D. Alexander Kann,[6] Darach Watson,[2] Michał J. Michałowski,[2] Andrew S. Fruchter,[7] Andrew J. Levan,[8] Jens Hjorth,[2] and Jesper Sollerman[2,3]

Received 2007 March 15; accepted 2007 December 18

ABSTRACT

GRB 060505 was the first well-observed nearby possible long-duration gamma-ray burst (GRB) that had no associated supernova. Here we present spatially resolved spectra of the host galaxy of GRB 060505, an Sbc spiral, at redshift $z = 0.0889$. The GRB occurred inside a star-forming region in the northern spiral arm at 6.5 kpc from the center. From the position of the emission lines, we determine a maximum rotational velocity for the galaxy of $v \sim 212$ km s^{-1}, corresponding to a mass of $1.14 \times 10^{11}\ M_{\odot}$ within 11 kpc from the center. By fitting single-age spectral synthesis models to the stellar continuum, we derive a very young age for the GRB site, confirmed by photometric and Hα line measurements, of around ~6 Myr, which corresponds to the lifetime of a 32 $M_{\odot}$ star. The metallicity derived from several emission-line measurements varies throughout the galaxy and is lowest at the GRB site. Using the Two Degree Field Galaxy Redshift Survey we can locate the host galaxy in its large-scale (~Mpc) environment. The galaxy lies in the foreground of a filamentary overdensity, extending southwest from the galaxy cluster Abell 3837 at $z = 0.0896$. The properties of the GRB site are similar to those found for other long-duration GRB host galaxies with high specific star formation rate and low metallicity, which is an indication that GRB 060505 originated from a young, massive star that died without making a supernova.

Subject headings: galaxies: abundances — galaxies: ISM — gamma rays: bursts

Online material: color figures

1. INTRODUCTION

GRB 060505 reinitiated the discussion on the connection between long gamma-ray bursts (GRBs) and core-collapse supernovae (SNe) as established with the detection of a SN spectrum in the afterglow of GRB 030329 (Hjorth et al. 2003; Stanek et al. 2003), of which all were classified as SNe Ic. Despite intense photometric and spectroscopic searches, no sign of a SN was detected for the nearby GRBs 060505 and 060614 (Fynbo et al. 2006; Gal-Yam et al. 2006; Della Valle et al. 2006). This raised the question of whether all long GRBs are accompanied by SNe (Zeh et al. 2004), or whether our understanding of the explosion mechanism is incomplete (Gehrels et al. 2006; Fryer et al. 2006; King et al. 2007; Zhang et al. 2007).

The *Swift* satellite (Gehrels et al. 2004) detected GRB 060505 on 2006 May 5, 06:36:01 UT, which had a fluence of $(6.2 \pm 1.1) \times 10^{-7}$ ergs cm^{-2} (Hullinger et al. 2006). With a duration of $T_{90} = 4$ s and a statistically significant spectral lag measured from *Suzaku* data (McBreen et al. 2007) it falls in the class of long-duration GRBs. The satellite did not, however, slew automatically, as the GRB was too faint to be detected in flight (Palmer et al. 2006) due to a high background caused by approaching the South Atlantic Anomaly. One of the two X-ray sources inside the Burst Alert Telescope error circle detected by the X-Ray Telescope (XRT) was finally established to be fading (Conciatore et al. 2006). An optical afterglow (Ofek et al. 2006) was found 1.5″ from the center of the revised XRT error circle with a radius of 2.5″ (Butler 2007), thereby localizing GRB 060505 to a region 4.3″ north of the center of the Two Degree Field Galaxy Redshift Survey (2dFGRS) spiral galaxy TGS 173Z112 at a redshift of $z = 0.089$. Later imaging and spectroscopy established the burst position to be coincident with a bright, compact star-forming region in one of the spiral arms of the host galaxy (Thöne et al. 2006; Fynbo et al. 2006), which was revealed to be a late-type, strong emission-line galaxy from the 2dFGRS data (Colless et al. 2001).

Host galaxies of GRBs are usually too distant to allow spatially resolved analysis with ground-based observations. Therefore, we only have information on the global properties of the galaxies, which appear to be mostly young, irregular, star-forming dwarf galaxies (Le Floc'h et al. 2003; Christensen et al. 2004). However, we know very little about the properties of the actual explosion sites. A recent study of GRB hosts observed with the *Hubble Space Telescope* (*HST*; Fruchter et al. 2006), which spatially resolved the host galaxies of 42 long GRBs, showed that the explosion sites coincide with the brightest regions in their host galaxies. Only two GRB hosts could so far be well resolved from the ground, those of GRB 980425 (Sollerman et al. 2005) and GRB 020819 (Jakobsson et al. 2005), both being spiral galaxies. In both cases, the GRBs occurred close to H II regions in the spiral arms of their host galaxies, which supports the connection between long GRBs and the deaths of massive stars.

In this paper, we present deep observations of the host galaxy of GRB 060505 in order to compare the galaxy and the burst site with the host galaxies of other long GRBs and to explicate the

[1] Based on ESO-ToO proposal 077.D-0661 and ESO-LP proposal 177.A-0591.

[2] Dark Cosmology Centre, Niels Bohr Institute, University of Copenhagen, Juliane Maries Vej 30, 2100 Copenhagen Ø, Denmark; cthoene@dark-cosmology.dk.

[3] Stockholm Observatory, Department of Astronomy, AlbaNova, SE-10691, Stockholm, Sweden.

[4] Astronomical Institute "Anton Pannekoek," University of Amsterdam, Kruislaan 403, 1098 SJ Amsterdam, Netherlands.

[5] Instituto de Astrofísica de Andalucía (IAA-CSIC), P.O. Box 3004, E-18080 Granada, Spain.

[6] Thüringer Landessternwarte Tautenburg, Sternwarte 5, D-07778 Tautenburg, Germany.

[7] Space Telescope Science Institute, 3700 San Martin Drive, Baltimore, MD 21218.

[8] Department of Physics, University of Warwick, Coventry CV4 7AL, UK.

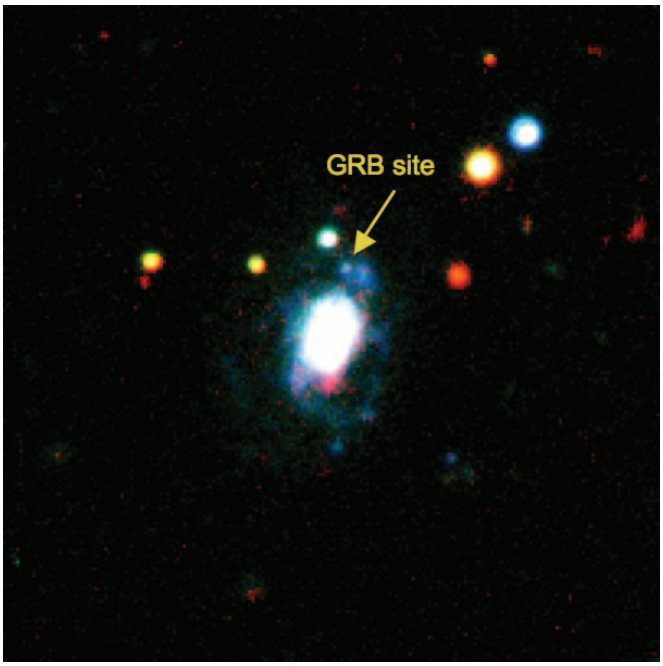

FIG. 1.—Color picture of the host galaxy of GRB 060505 from BRK_S bands, with field of view $40'' \times 40''$, north up, and east to the left; the position of the OT is marked.

controversial nature of this SN-less long-duration GRB. In § 2 we present spatially resolved spectroscopy of the host galaxy as well as photometric data. Section 3 describes the general properties of the galaxy, concerning the classification, photometry of the entire galaxy, colors, and mass determination, as well as dynamical measurements. In § 4 we examine the differences between several parts of the galaxy including the GRB site, the different stellar populations, and their ages, as well as differences in metallicity and extinction along the galaxy. The last section, finally, studies the large-scale structure around the host galaxy.

Throughout the paper we adopt a cosmology with $H_0 = 71$ km s^{-1} Mpc^{-1}, $\Omega_m = 0.27$, $\Omega_\Lambda = 0.73$. A redshift of $z = 0.0889$ then corresponds to a luminosity distance of 401 Mpc, and $1''$ corresponds to 1.64 kpc.

2. OBSERVATIONS

Spectra were taken with FORS2 at the Very Large Telescope (VLT) on Cerro Paranal in Chile on 2006 May 23, 18 days after the burst when there was no contribution from the afterglow. We used grism 300V, which covers the wavelength range 3500–9600 Å, and a $1.0''$ wide slit resulting in a nominal resolution of 11 Å full width at half-maximum (FWHM) or 590 km s^{-1} at $\lambda = 5600$ Å. Seeing conditions were decent with a seeing of $0.75''$ FWHM, determined from the acquisition image. In order to minimize the effects of atmospheric dispersion, the FORS instrument uses a so-called Longitudinal Atmospheric Dispersion Corrector (LADC), which reduces differential slit loss. We obtained two 1800 s and one 600 s exposures, which were combined and reduced with standard packages in IRAF. The dispersion solution used for the wavelength calibration had an rms of about 0.1 Å.

The co-added two-dimensional spectrum was divided into four pieces of 8 and one piece of 9 pixels width along the spatial direction, where 1 pixel corresponds to $0.25''$ or 0.41 kpc at the redshift of the galaxy. These five parts represent distinct regions in the galaxy such as the spiral arms and the GRB site covered by the slit (see Figs. 1, 2, and 4). We used the continuum of the bulge which has the brightest trace to create a "template" trace and extract all five pieces using the same trace function, in order to account for the bending of the trace toward the blue. The individual parts were then flux calibrated with IRAF using observations of the spectrophotometric standard star LTT 7379 from 2006 April 2, which was taken under photometric conditions. Cross-calibration with observations of the standard star LTT 1788 on August 17 gave consistent results for the fluxes. We estimate the error of the flux calibration to be around 10% in the wavelength range between 4000 and 7500 Å, which covers the range of the host galaxy emission lines. The flux calibration obtained in such a way can, however, only serve as a relative flux calibration and to determine the shape of the continuum.

Imaging was obtained with FORS1 at the VLT in the *BVRIz* bands on 2006 September 14 and in the *U* band on 2006 October 1 under photometric conditions. Images in the K_S band were taken with ISAAC at the VLT on September 24. The images of FORS1 VLT in *UBVRI* were calibrated using photometric zero points from the same night as the observations in the corresponding bands. For the *z* band, which has no zero points available, we calibrated a standard field observed on the same night with magnitudes from Sloan Digital Sky Survey observations of the same field, which was then used to derive instrumental zero points in the *z* band. The K_S-band image was calibrated using a comparison star in the same field from the Two Micron All Sky Survey catalog (Skrutskie et al. 2006).

3. GLOBAL PROPERTIES OF THE GALAXY

3.1. *Classification*

The host galaxy of GRB 060505 is a late-type spiral galaxy with at least two major spiral arms; the GRB occurred in the northern arm of the galaxy (see Fig. 2). From the morphology and from the strength of the Hα, Hβ, and the forbidden nebular emission lines (see § 4), this galaxy can be classified as an Sbc spiral (Kennicutt 1992a). We detect Ca H and K absorption lines and the 4000 Å break; Ca H is, however, only clearly detected in the bulge region. The three other spiral host galaxies of long GRBs are also late-type spiral galaxies, with GRB 980425 occurring in an SBc spiral (Fynbo et al. 2000), GRB 990705 in an Sc (Le Floc'h et al. 2002), and GRB 020819 presumably in an Scd spiral galaxy (Jakobsson et al. 2005).

We determined the magnitudes of the entire host galaxy using the images in *UBVRIz* from FORS VLT and in K_S from ISAAC. In order to get the total flux of the host galaxy, aperture diameters of $15''$ were used for the *U* band, $12''$ for *BVRIz*, and $8.88''$ for the *K* band, which were the smallest sizes to contain the total flux. The different aperture sizes were determined from a curve-of-growth analysis for each band. The flux of the three stars inside the apertures contributing about 10% to the total flux was subtracted. These magnitudes and the corresponding colors are listed in Table 1; the magnitudes are corrected for the foreground extinction of $E(B-V) = 0.021$. From the *R*-band magnitude we derive an absolute magnitude for the host of $M_R = -20.15 \pm 0.02$ mag (no *K*-correction applied), which corresponds to $0.4L^*$ with $M_R^* = -21.21$ mag (Blanton et al. 2001) using $h = 0.71$. The colors of this galaxy are actually too blue for an Sbc spiral galaxy, but rather resemble the values for an irregular galaxy (Fukugita et al. 1995). Also, the equivalent widths (EWs) of the emission lines are generally stronger than expected for a normal Sbc spiral (Kennicutt 1992b).

A closer look at the morphology reveals some asymmetry in the spiral structure and distortions in the western part of the galaxy which can also be seen in the *HST* images of the host galaxy

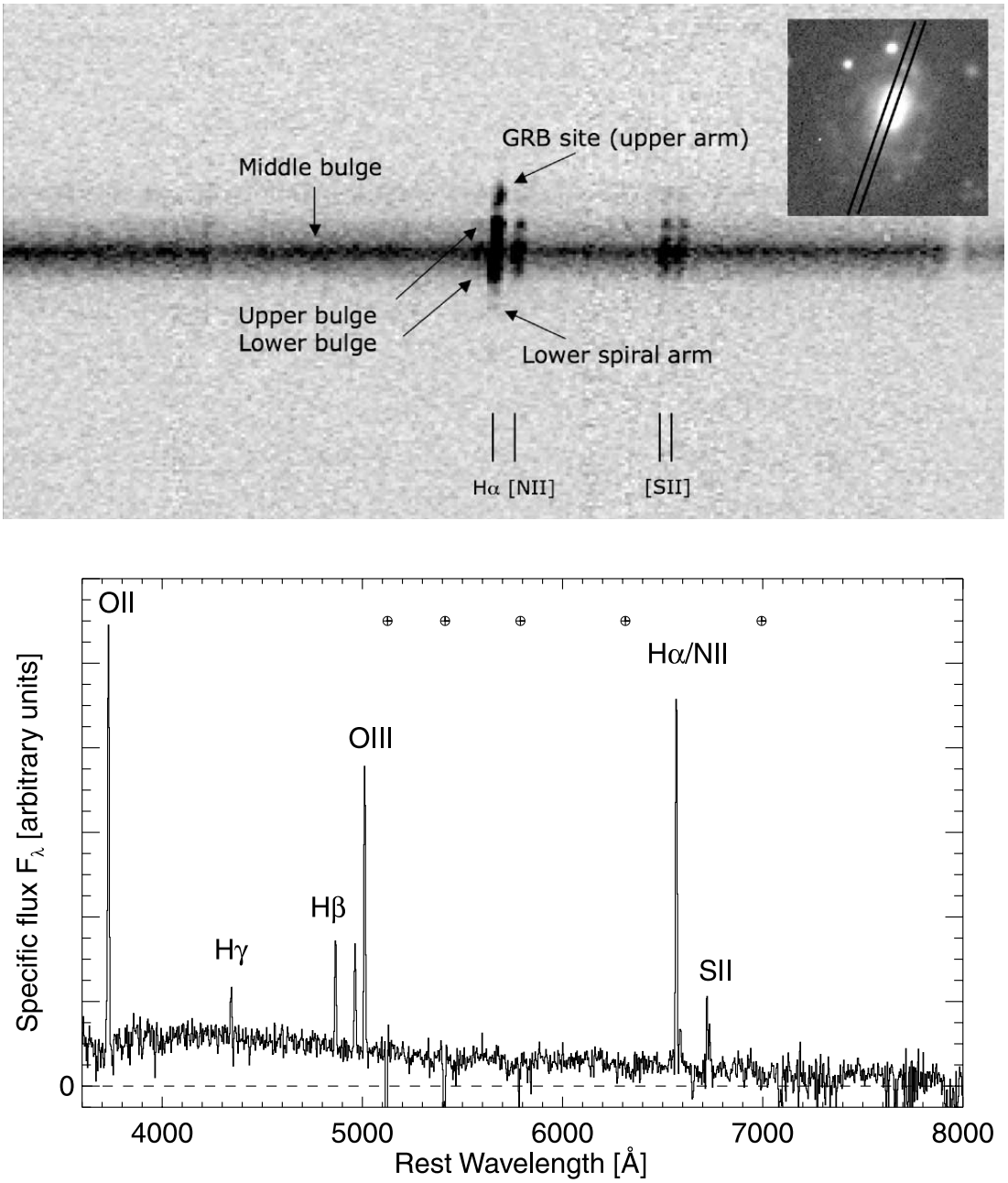

FIG. 2.—*Top*: Two-dimensional long-slit spectrum of the host galaxy of GRB 060505 around the Hα emission line. Indicated are the five parts that were extracted from the spectrum. The inset shows the position of the slit across the host galaxy. *Bottom*: One-dimensional spectrum at the GRB position; the crossed circles mark telluric lines. [*See the electronic edition of the Journal for a color version of this figure.*]

presented in Ofek et al. (2007; see also Fig. 5). This suggests a recent minor merger event which could have triggered the excess star formation in parts of the host, which overall has an older stellar population (see § 4.3). It might also explain the deviation of the colors and emission-line strengths compared to usual Sbc spiral galaxies.

3.2. *Measurement of the Rotation Curve*

In order to measure the rotation curve of the host galaxy, the four brightest emission lines in the two-dimensional spectrum were used, namely [O II], Hβ, [O III] λ5008, and Hα (see Fig. 2). A two-dimensional continuum-subtracted postage stamp spectrum was produced for each emission line, with the continuum being modeled as a linear function fitted near each emission line. For each spatial point along the slit, the postage stamp spectrum, a Gaussian was fitted using the IRAF task `ngaussfit` from the STSDAS package. At first the FWHM was kept as a free parameter, resulting in a typical value of 9 Å. The FWHM was then fixed at 9 Å, and a Gaussian was fitted again to each row, now with only two free parameters, the center (i.e., observed wavelength) and amplitude. Uncertainties on the fitted parameters were calculated using `ngaussfit`, based on an input noise spectrum which was calculated as photon noise and readout noise from the two-dimensional galaxy spectrum before sky subtraction.

The fitted observed wavelengths $\lambda_{\rm obs}$ were first corrected for a zero-point error in the wavelength calibration and then used to calculate rest-frame line-of-sight velocities as $v_{\rm rest}^{\rm los} = c(z - z_{\rm sys})/(1 + z_{\rm sys})$, with $z = \lambda_{\rm obs}/\lambda_{\rm rest} - 1$, where a systemic redshift of $z_{\rm sys} = 0.0889$ was used. The velocities were finally corrected for inclination (deprojected velocities) as $v_{\rm rest}^{\rm deproj.} = v_{\rm rest}^{\rm los}/\sin i$, with i

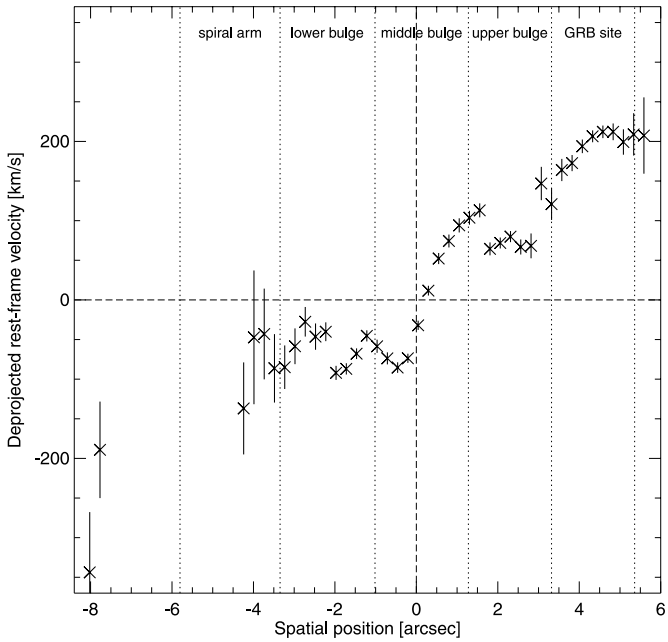

FIG. 3.—Rotation curve using the weighted mean of the center of the emission lines [O II], Hβ, [O III], and Hα over the spatially resolved host galaxy spectrum. The curve shows the true rotation curve of the galaxy, corrected for the inclination of 49°. [*See the electronic edition of the Journal for a color version of this figure.*]

being the inclination (see § 3.3). The row number in each postage stamp spectrum was transformed into a spatial coordinate with respect to the continuum center. The location of the continuum center as a function of observed wavelength (the "trace" of the continuum) was measured in a number of bins in an aperture of width 14 pixels = 3.5″ and fitted using a linear function. The used systemic redshift was chosen so that the median velocity of the 16 data points (4 per emission line) located within ±0.5″ of the continuum center was zero; therefore, the calculated velocities were defined to be zero at the continuum center.

To plot the rotation curve we only use points for which the fitted Gaussian amplitude was larger than 3 times its uncertainty. The rotation curves based on the four emission lines agreed reasonably well, although there were places where the difference was larger than the calculated uncertainties could explain. The weighted mean rotation curve shown in Figure 3 was calculated using inverse variance weighting.

3.3. *Galaxy Size and Mass*

In order to determine the inclination of the galaxy, we measured the ellipticity of the disk with SExtractor (Bertin & Arnouts 1996) using the photometric data in the *V*, *R*, and *I* bands. We find $e = 0.346 \pm 0.006$, which gives an inclination of $49^\circ \pm 1^\circ$. The radius of the circle containing 80% of the light is about 4.3″, which corresponds to a line-of-sight radius of ∼11 kpc.

Furthermore, we determined the stellar and baryonic mass of the galaxy by fitting empirical models for GRB host galaxies to the spectral energy distribution (SED) of the galaxy according to Michałowski et al. (2008). This method is based on the radiative transfer code GRASIL developed by Silva et al. (1998), which

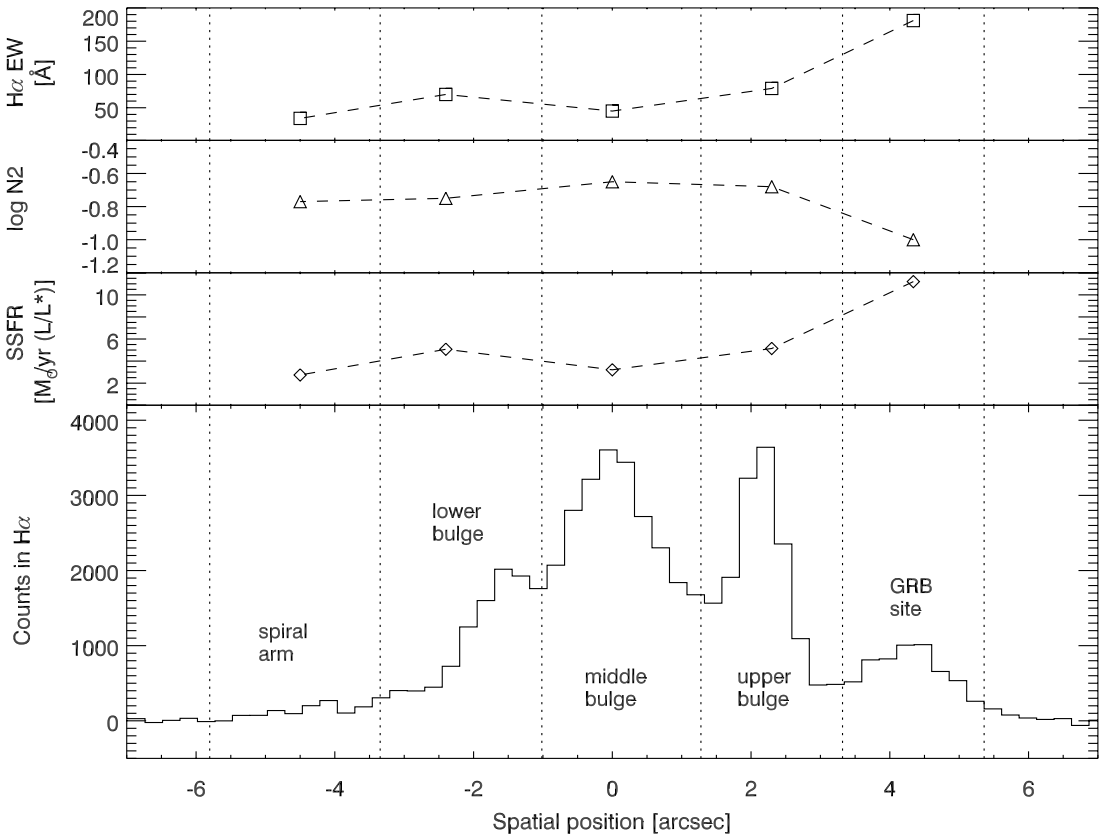

FIG. 4.—*Bottom*: Cut through the spectrum along the Hα line and indication of the regions selected for the individual spectra (see also Fig. 2). The upper three panels show the specific SFR per luminosity, the metallicity proxy using the N2 parameter N2 = log([N II]/Hα) as described in § 4.4, and the Hα EW as a proxy for the maximum age of the youngest stellar population in the five parts of the spectrum (the higher the EW, the younger the population). All three panels show that the GRB site is considerably different from the rest of the host galaxy. [*See the electronic edition of the Journal for a color version of this figure.*]

TABLE 1
PHOTOMETRY OF THE HOST GALAXY

Filter	Magnitude	Color	Magnitude
U	18.43 ± 0.05	...	...
B	18.89 ± 0.02	$U-B$	−0.46 ± 0.05
V	18.27 ± 0.02	$B-V$	0.62 ± 0.03
R	17.90 ± 0.02	$V-R$	0.37 ± 0.03
I	17.51 ± 0.02	$R-I$	0.39 ± 0.03
z	17.29 ± 0.08	$R-z$	0.59 ± 0.08
K	15.85 ± 0.04	$R-K$	2.05 ± 0.04

NOTES.—Magnitudes given are in the Vega system. The values are corrected for the foreground extinction of $A_V = 0.06$.

models the spectrum of the galaxy taking the stellar UV output and its absorption and redistribution by dust. The best-fitting model was found to be similar to the SED of the GRB 000210 host galaxy, which then gives a total stellar mass of $(7.9 \pm 0.4) \times 10^9\ M_\odot$ and a total baryonic mass of 2 times the stellar mass. The error quoted comes only from the errors of the model fitting; the total error from the model itself is around a factor of 2. The measurement of the rotation curve which flattens at a value of 212 km s^{-1} (considering the inclination) allows an estimate of the dynamical mass to $1.14 \times 10^{11}\ M_\odot$ within a radius of 11 kpc.

4. SPATIALLY RESOLVED PROPERTIES

Figure 4 shows the different regions selected for the analysis of the properties in different parts of the galaxy. The three peaks in Hα within the bulge seem to come from the nucleus of the galaxy and the innermost regions of the two spiral arms, as can be seen in Figure 2. The region in the upper spiral arm around the site where the GRB occurred is a large H II region, representing a clear peak in the Hα spatial profile. A second H II region is to the west of the GRB position, just outside the slit. The spiral arm below the bulge only has a very weak peak in Hα, which indicates a low star formation rate in this region.

We analyze the properties of the interstellar medium (ISM) in the individual regions by comparing the emission-line fluxes from the different regions (see Table 2). The Balmer lines Hα, Hβ, and Hγ were found in emission in all regions, except that Hγ was not detected in the faint spectrum of the lower spiral arm. We also detect the forbidden lines [O II] $\lambda\lambda$3727, 3729 and [O III] $\lambda\lambda$5007, 4959, as well as [N II] λ6568 and the [S II] $\lambda\lambda$6716, 6731 doublet. We measured the line properties (see Table 2) using the `splot` task in IRAF, which fits a Gaussian to the lines. The lines are unresolved within the resolution of the instrument. The continuum has been corrected for the Galactic extinction of $E(B-V) = 0.021$ mag; measured fluxes were then both corrected for the underlying stellar absorption and extinction in the host galaxy.

4.1. *Burst Location*

The accurate location within the host galaxy could be determined for only a small number of bursts. For XRF 020903 it was shown that the GRB occurred close to, but not inside, a massive, star-forming supercluster (Bersier et al. 2006; Le Floc'h et al. 2006; Soderberg et al. 2004). GRB 980425 was coincident with a smaller star-forming region (Fynbo et al. 2000; Sollerman et al. 2002). GRB 990705, whose spiral host could be resolved in *HST* images, also occurred close to a star-forming region within a spiral arm (Le Floc'h et al. 2002). GRB 020819 lies close to a brighter "blob," possibly a star-forming region, next to a face-on spiral galaxy, whose connection to the spiral galaxy has yet to be proven spectroscopically (Jakobsson et al. 2005).

HST images of the host galaxy (Ofek et al. 2007) show clearly that the burst lies at the edge of an H II region with a size of 400 pc. We have reanalyzed these *HST* images, which are now public, taken in the F475W filter on 2006 May 19 (*HST* program 10551, PI: S. R. Kulkarni). Performing astrometry relative to the VLT observations taken on May 5, we find that our position (see Fig. 5) differs slightly from that of Ofek et al. (2007), but is consistent within the errors on each measurement. Following the method of Fruchter et al. (2006) we determine that the burst occurred at the 80th percentile of the host galaxy light (i.e., 80% of the light of the host galaxy is contained in pixels of lower surface brightness than that containing the burst), which is close to the median observed for long-duration GRBs. The difference in the values obtained by us and Ofek et al. (2007) comes from the slightly differing astrometry and the application of a small convolution to the image to allow for the positional uncertainty in our analysis. We note, however, that both our and Ofek's positions are consistent with the peak of the nearby H II region, which is one of the brightest regions of the galaxy. The peak of the light of this region lies at the 96th percentile of the galaxy light distribution.

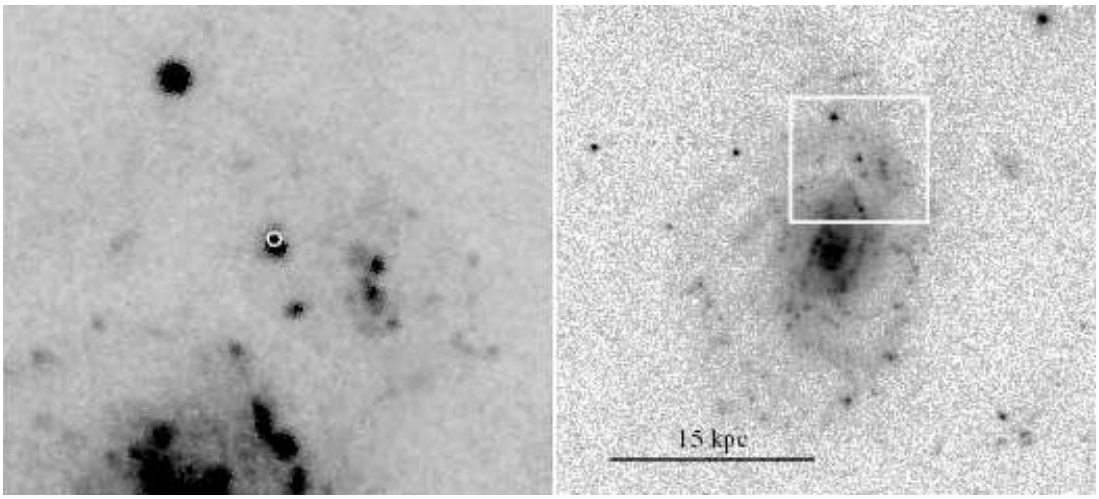

FIG. 5.—*HST* image of the host galaxy of GRB 060505 (*right*) and a smaller region showing the H II region at the position of the GRB (*left*); the optical afterglow position from ground-based observations is indicated by the white circle.

TABLE 2
Emission Lines in Different Parts of the GRB 060505 Host Galaxy

Line	Site	λ_{obs} (Å)	EW (Å)	Flux (corr.) (10^{-17} ergs cm^{-2} s^{-1} Å^{-1})
[O II] $\lambda\lambda$3727, 3729	GRB	4064.6	−152.3	11.2 ± 0.2
	Bu	4063.2	−97.9	12.7 ± 0.3
	Bm	4062.9	−48.91	16.8 ± 0.4
	Bl	4061.8	−56.38	13.4 ± 0.4
	lS	4061.5	−43.83	2.87 ± 0.08
Hγ λ4340	GRB	4731.6	−9.82	1.12 ± 0.02
	Bu	4730.5	−6.85	1.45 ± 0.03
	Bm	4731.0	−1.796	0.99 ± 0.03
	Bl	4729.4	−2.598	0.86 ± 0.03
	lS	...	...	...
Hβ λ4861	GRB	5299.9	−39.20	2.98 ± 0.02
	Bu	5298.3	−27.22	4.53 ± 0.02
	Bm	5297.1	−8.064	4.27 ± 0.03
	Bl	5296.3	−12.60	3.35 ± 0.02
	lS	5297.9	−8.917	0.65 ± 0.02
[O III] λ4959	GRB	5406.4	−36.31	2.84 ± 0.18
	Bu	5404.4	−11.32	2.27 ± 0.20
	Bm	5402.9	−4.016	2.19 ± 0.13
	Bl	5402.8	−5.758	1.64 ± 0.12
	lS	5403.4	−6.004	0.43 ± 0.03
[O III] λ5007	GRB	5458.6	−92.80	7.20 ± 0.06
	Bu	5456.4	−40.46	7.84 ± 0.14
	Bm	5456.3	−9.709	5.17 ± 0.13
	Bl	5455.1	−17.70	4.85 ± 0.13
	lS	5454.2	−21.75	1.43 ± 0.08
Hα λ6567	GRB	7154.2	−181.8	9.73 ± 0.03
	Bu	7152.6	−79.32	12.1 ± 0.06
	Bm	7150.6	−45.71	21.9 ± 0.09
	Bl	7149.6	−70.33	12.9 ± 0.04
	lS	7150.1	−34.70	1.59 ± 0.02
[N II] λ6586	GRB	7175.8	−19.44	0.96 ± 0.03
	Bu	7174.5	−16.45	2.53 ± 0.06
	Bm	7172.7	−10.62	4.97 ± 0.09
	Bl	7172.3	−13.08	2.28 ± 0.04
	lS	7175.4	−6.142	0.27 ± 0.03
[S II] λ6716	GRB	7321.1	−50.81	1.60 ± 0.04
	Bu	7319.3	−23.04	3.04 ± 0.05
	Bm	7318.1	−10.55	4.58 ± 0.03
	Bl	7317.4	−14.57	2.34 ± 0.03
	lS	7316.2	−29.42	0.77 ± 0.12
[S II] λ6731	GRB	7335.6	−36.25	1.09 ± 0.04
	Bu	7334.4	−20.25	2.64 ± 0.05
	Bm	7332.7	−7.164	3.10 ± 0.03
	Bl	7331.9	−9.370	1.48 ± 0.03
	lS	7334.5	−36.05	0.91 ± 0.12

Notes.—Abbreviations for the different parts along the slit: GRB = GRB explosion site; bu = upper part of the bulge; bm = middle part; bl = lower part; ls = lower spiral arm. Observed wavelengths are not corrected for the zero-point error of around 4 Å mentioned in § 3.2. The fluxes are only corrected for the Galactic extinction of $E(B-V) = 0.021$ mag before measuring the fluxes; no extinction correction in the host galaxy has been applied due to its uncertainty (see § 4.2). The errors in the fluxes do not include the overall error from the flux calibration, which is around 10%.

The absolute magnitude (−19.6 mag) and physical size of the galaxy (R_{80}) are slightly larger and brighter than the mean of long-duration GRB hosts studied by Fruchter et al. (2006), but fit comfortably within the observed range.

The position of GRB 060505 within the host makes it unlikely that the GRB was a chance superposition with the galaxy and in fact occurred at a higher redshift, which could have been an explanation for the lack of the detection of a SN. This clear association of the optical transient (OT) position with a star-forming region also supports the suggestion that GRB 060505 was due to the collapse of a massive star that originated in this star-forming region. Short bursts have also been found in star-forming galaxies (Berger et al. 2007), but a clear association with a star-forming region has not been possible so far.

4.2. *Extinction*

Another issue in the discussion about the absent SN in the light curve of GRB 060505 is the question of extinction along the line of sight. The Galactic extinction along the line of sight of the GRB determined from the sky maps of Schlegel et al. (1998)

TABLE 3
PHOTOMETRY OF THE GRB SITE AND THE NEARBY H II REGION WEST OF THE GRB SITE

Filter	GRB Site (mag)	H II Region (mag)
B	24.31 ± 0.13	24.50 ± 0.08
V	23.99 ± 0.09	24.10 ± 0.08
R	23.84 ± 0.07	24.15 ± 0.16
I	23.53 ± 0.15	23.45 ± 0.08
K_S	21.95 ± 0.30	...

NOTES.—Magnitudes given are in the Vega system. The values are corrected for the foreground extinction of $A_V = 0.06$.

is very low, with $E(B - V) = 0.021$ mag. Determining the extinction in the individual parts in the host galaxy is difficult because of the uncertainty in the possible Balmer absorption by an underlying older population, which might especially play a role in the innermost parts of the host galaxy. For the following analysis of the properties in the different parts, we mainly used emission-line ratios so that extinction correction plays a minor role.

For the GRB region, we determined the extinction from the broadband afterglow photometry using the values of the afterglow from the series of observations in the *B*, *V*, *R*, and *I* bands from the first night with the contribution of the galaxy subtracted (D. Xu et al. 2008, in preparation). The SED gives no indication of additional reddening along the line of sight through the galaxy, and the slope is consistent, within errors, with X-ray data from *Swift* XRT observations. This rules out the possibility that GRB 060505 was obscured by dust which would have prevented the detection of a SN. Furthermore, this argues against the suggestion that GRB 060505 took place at a higher redshift and just happened to lie by chance behind this star-forming region, as this would probably have added additional extinction to the SED.

4.3. *Stellar Population Modeling of the GRB Site*

The age of the stellar population at the GRB site is an important key to understand the progenitor nature of this SN-less GRB. We analyze the burst region with photometry for the H II region of the GRB using an aperture of radius 0.4″ and a sky annulus from 0.6″ to 1.0″. The small aperture was necessary, since the GRB occurred in the spiral arm of the galaxy. All the images had similar seeing except for the *I* and K_S bands, which were smoothed to the resolution of the *BVR* images before the photometry was extracted. Aperture corrections were determined from isolated, well-exposed but nonsaturated stars in the science images. The photometry was corrected for Galactic extinction. We did a similar analysis for the other H II region to the west of the GRB site in the same spiral arm, which was outside the slit, in order to investigate a possible connection between the two regions in terms of their ages. The photometry of these two H II regions is presented in Table 3. For the second H II region, the signal in the K_S band was too low to derive any magnitude.

The photometric results were then compared to predictions from the spectral evolutionary synthesis models of Zackrisson et al. (2001). These models include a realistic treatment of the nebular line and continuum emission, which has been found to be important for modeling photometric data of young stellar populations (Östlin et al. 2003, 2007), where the nebular component may significantly affect the broadband colors. We have redshifted the spectra from the Zackrisson et al. (2001) model, integrated over the instrument throughput curve, and fitted these to the observed photometry. We adopted an instantaneous burst with Salpeter initial mass function (IMF) from 0.08 to 120 $M_\odot$, and two different metallicities for the stars and gas of $Z = 0.004$ [$12 + \log(\mathrm{O/H}) \sim 8.0$ of 0.2 $Z_\odot$] and $Z = 0.008$ [$12 + \log(\mathrm{O/H}) \sim 8.3$ or 0.4 $Z_\odot$]. For the extinction we used a Galactic extinction law (Cardelli et al. 1989). One degree of freedom, namely the dust reddening, can be removed from the fit, as both Hα and Hβ are available from the spectrum. In order to correct for the underlying Balmer absorption before deriving the extinction, we use the models of Gonzales Delgado et al. (1997).

The best fits were obtained with a metallicity of $Z = 0.008$, giving an age of 9 Myr and a reddening of $E(B - V) = 0.07$ mag. It should be noted, however, that in addition to an interval around 9 Myr (7–14 Myr), the 1 σ uncertainties also allow solutions in the range 25–100 Myr. A lower metallicity of $Z = 0.004$ gives a worse fit, and the only allowed interval within the 1 σ limit is 25–65 Myr. In conclusion, although favoring a young progenitor, the broadband photometry in this case does not provide very tight constraints on the stellar population age. The modeling for the H II region west of the GRB site gave an even lower age of 3–5 Myr, applying an extinction of $E(B - V) = 0.25$ mag. Here the extinction was left as a free parameter, since no spectrum covering this region was available. Even though we lack a more robust measurement of the age of this region from, for example, spectroscopic measurements of the Hα EW, our data suggest that these two H II regions are different from the rest of the galaxy, and that their onset of star formation might indeed have been triggered at approximately the same time by a minor merging event, as suggested in § 3.1.

An important indicator for the age of a population, especially when it is very young, is the predicted evolution of the Hα EW derived from the spectra. Assuming again a Salpeter IMF from 0.08 to 120 $M_\odot$ and a metallicity of $Z = 0.008$, the EW of ~192 Å indicates an age of 6 ± 1 Myr or less at the GRB site based on the evolution of the EW derived by Zackrisson et al. (2001). This age has to be interpreted as an upper limit due to the H I covering factor leading to a possible Lyman continuum leak, which could lower the strengths of the Hα line. The measurement of the Hα EW is not affected by calibration errors and very reliable in terms of its physical origin, as it is directly related to the percentage of very young, blue stars in the region. In order to illustrate the relative difference of the stellar population age throughout the galaxy, we plot the Hα EW in Figure 4, which is inversely proportional to the age of the population as a proxy for the maximum age of the youngest stellar population.

The different methods applied for the GRB region agree in a young age for the underlying population. The age derived from the Hα EW is most reliable from the calibration point of view, as photometry of the GRB region is always affected by contamination from neighboring regions. Both methods point to a very low age of the progenitor star of about 6 Myr, which corresponds to the lifetime of a 32 $M_\odot$ star. A further determination of a young age of the GRB region could be done by directly detecting the presence of Wolf-Rayet (WR) stars (Wiersema et al. 2007). Unfortunately, the continuum flux of our spectrum is not high enough to detect WR star lines. The young ages found for this region, however, connect well with predictions from the latest stellar evolution models for the lifetimes of massive, rapidly rotating, chemically homogeneous single-star progenitors (Yoon & Langer 2005; Woosley & Heger 2005).

4.4. *Metallicity*

In order to determine the metallicity, we used the R_{23} parameter (first proposed by Pagel et al. 1979), which is a two-valued

TABLE 4
METALLICITIES IN THE DIFFERENT PARTS IN $12 + \log(O/H)$

Site	R_{23} K07 (lb/ub)	O3N2	N2/metal.
GRB	7.96/8.20	8.29	−1.00/8.28
Upper bulge	7.69/8.44	8.44	−0.68/8.47
Middle bulge	7.84/8.36	8.50	−0.65/8.50
Lower bulge	7.87/8.34	8.44	−0.75/8.42
Lower spiral arm	8.00/8.18	8.38	−0.77/8.41

NOTES.—K07 refers to Kewley et al. (2007); ub and lb stand for upper and lower branch solution of the two-valued R_{23} parameter. The last column states the N2 parameter and the metallicity derived from it according to Pettini & Pagel (2004).

TABLE 5
STAR FORMATION RATE IN THE DIFFERENT PARTS

Site	SFR/8 pixels ($M_\odot$ yr^{-1})	M_B	Luminosity-weighted SFR [$M_\odot$ yr$^{-1}(L/L_*)^{-1}$]
GRB	0.015	−13.82	11.2
Upper bulge	0.018	−14.86	5.14
Middle bulge	0.033	−16.03	3.21
Lower bulge	0.020	−14.99	5.07
Lower Spiral arm	0.003	−13.60	2.74

NOTE.—The M_B is the absolute magnitude of the corresponding region in B band (observer frame).

function of the metallicity. The degeneracy between the two solutions can be broken by using the ratio [N II]/Hα (Lilly et al. 2003), which indicates some preference for the lower branch solution for the GRB site with [N II]/H$\alpha = 0.10$ and likely a preference for the upper branch in the other parts of the galaxy; however, an upper branch solution for all regions cannot be excluded. In recent years, a number of recalibrations of the R_{23} parameter have been done. Most of the recent metallicities of GRB host galaxies have been determined using the parameterization of Kewley & Dopita (2002) for the two branches, which takes into account the oxygen ionization state. Using a first guess for the metallicity and a decision for the upper or lower branch solution, the metallicity then can be determined iteratively, which usually converges very quickly. Recently, a new recalibration has been done by Kewley et al. (2007), which corrects for the known overestimation of the metallicity from the R_{23} parameter using metallicity calibrations based on measurement of the electron temperature T_e. In Table 4 we only give the values from the recent Kewley et al. (2007) calibration and the solution from both branches.

An independent estimate for the metallicity comes from the so-called O3N2 method using the ratio O3N2 = log[(O III/Hβ)/(N II/Hα)] (e.g., Pettini & Pagel 2004), which is empirically calibrated on a sample of H II regions with electron temperature (T_e) determined metallicities. This parameter is less sensitive to extinction compared to the R_{23} parameter, as both line ratios lie very close to each other and are therefore very little affected by extinction. Adopting the metallicities determined through the O3N2 parameter as $12 + \log(O/H) = (8.73–0.32)$O3N2, the gradient throughout the host galaxy is slightly less pronounced compared to the estimate through the R_{23} method, but the tendency is consistent with the values derived from R_{23}.

A final relative metallicity estimator is the N2 parameter, which is simply log([N II]/Hα) (Pettini & Pagel 2004). This ratio is insensitive to underlying extinction due to the small wavelength difference between the two lines. The calibrations by Pettini & Pagel (2004) allow us to transform this ratio into an oxygen abundance. The N2 parameter and the derived metallicity show a picture consistent with the metallicity derived with the R_{23} and O3N2 parameter. Again, we find a relatively low metallicity in the GRB region and a higher one in the other parts of the galaxy. In Figure 4 we therefore plot the N2 parameter as a proxy for the relative metallicity.

Consistently for all methods, we find that the metallicity varies over the different regions in the host galaxy (see Table 4 and Fig. 4 for the [N II]/Hα proxy). The star-forming region at the GRB site has a relatively low value (0.19–0.40 $Z_\odot$ for the different calibrations and taking 8.69 as the value for the solar metallicity; Asplund et al. 2004), whereas in the other regions covered by the slit the metallicity ranges from 0.49 solar at lower spiral arm to 0.65 solar in the middle bulge region. Here, we also have a much older stellar population, which could be responsible for the enrichment of the ISM in that part of the galaxy. From the O3N2 and N2 calibrations, we can infer a (O/H) metallicity gradient throughout the galaxy of −0.03 dex kpc^{-1}. For the R_{23} parameter, we cannot determine the gradient, as the decision for the upper or lower branch solution in the different regions remains unclear. For comparison in the local universe, for the Milky Way, M33, and M51 gradients of −0.07 (Smartt & Rolleston 1997), −0.05 (Magrini et al. 2007), and −0.02 dex kpc^{-1} (Bresolin et al. 2004) have been derived.

4.5. *Luminosity-weighted Star Formation Rate*

The instantaneous star formation rate (SFR) can be obtained from the Hα emission flux, as H I is excited by UV light mainly coming from young, blue O stars which have their peak luminosity in the UV. The conversion formula for Hα is then SFR$[M_\odot\ \mathrm{yr}^{-1}] = 7.9 \times 10^{-42} 4\pi\Phi[\mathrm{ergs\ cm^2\ s^{-1}}] d_L^2$ (Kennicutt 1998), where d_L is the luminosity distance and Φ is the Hα line flux.

As we only cover a part of the galaxy by the slit, we cannot make a statement about the global SFR in this spiral galaxy, but only about the relative SFR between the different parts that we extracted from the spectrum. Table 4 lists the SFR per 8×5 pixels along the slit (the area covered by the individual parts of the two-dimensional spectrum), which corresponds to an area of 3.28×2.05 kpc^2. We then scale the SFR to the B-band luminosity fraction compared to the luminosity of a "standard" galaxy of $M_B = -21$ mag (Christensen et al. 2004) to get the luminosity-weighted SFR for the individual regions. For the B-band magnitudes of the parts corresponding to the individual spectra, we determine the magnitude in a rectangular aperture of 8×5 pixels (9×5 for the lower spiral arm) from the VLT host image at the same position as the spectrum pieces (see Table 5 and Fig. 4). The luminosity-weighted SFR is a factor of 2–3 higher in the star-forming region around the GRB site with 11 $M_\odot$ yr$^{-1}(L/L_*)^{-1}$, compared to the value in the bulge of around 3–5 $M_\odot$ yr$^{-1}(L/L_*)^{-1}$. The latter value is higher than in an average spiral galaxy (Kennicutt 1998) and a factor of 8 higher than in the spiral arm at the opposite side of the galaxy, which has 2.7 $M_\odot$ yr$^{-1}(L/L_*)^{-1}$. The luminosity-weighted SFR at the GRB site, however, fits very well into the average value found in GRB host galaxies of 9.7 $M_\odot$ yr$^{-1}(L/L_*)^{-1}$ (Christensen et al. 2004). To determine an absolute value for the SFR is, however, difficult, as the absolute flux calibration might not be fully reliable. In addition, the B band of our Galaxy is shifted slightly toward the V band, so the absolute magnitude in rest-frame B band would be smaller, and therefore the luminosity-weighted SFR slightly lower.

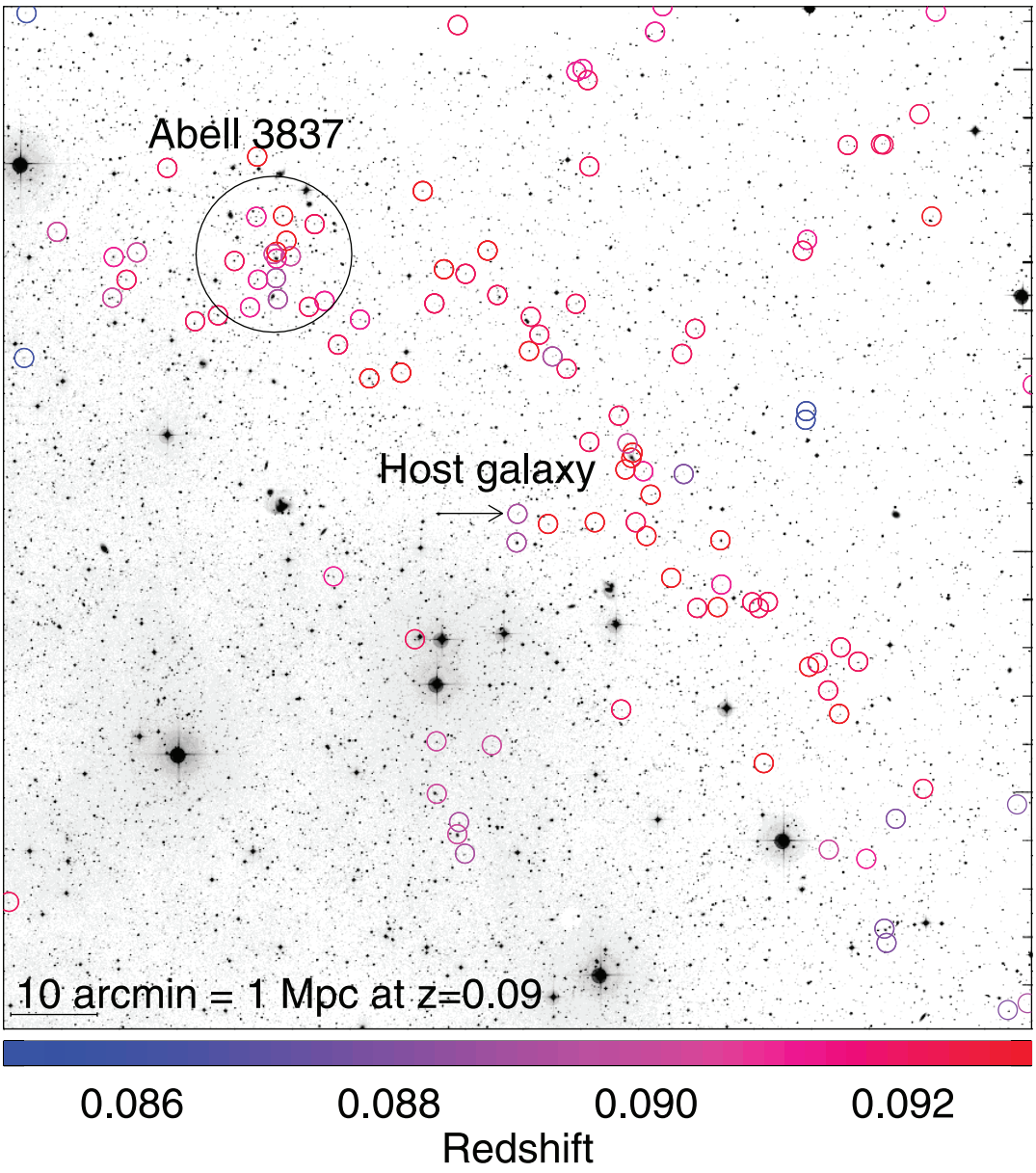

FIG. 6.—Large-scale structure around the host galaxy of GRB 060505 shown in a field of size $2^\circ \times 2^\circ$. The colored circles indicate the galaxies with redshifts known from the 2dF galaxy survey. Blue indicates galaxies with a lower redshift compared to the host galaxy; red indicates a higher redshift. Most galaxies in the field lie on a filament at slightly higher redshift than the host galaxy, stretching out from the Abell 3837 cluster to the northeast of the host.

5. THE LARGE-SCALE STRUCTURE AROUND THE GRB HOST GALAXY

The fact that the field of GRB 060505 is covered by the 2dF survey (Colless et al. 2001) allows us to study the large-scale structure around it.

The galactic environments of GRBs have so far not been studied much. At low redshifts Foley et al. (2006) studied the field of the host galaxy of GRB 980425, which was reported to be a member of a group. However, based on redshift measurements of the proposed group members, Foley et al. (2006) could establish that the host of GRB 980425 is an isolated dwarf galaxy. Levan et al. (2006) also proposed GRB 030115 to be connected to a cluster around $z \sim 2.5$ based on photometric redshifts. At redshifts $z \gtrsim 2$ a few GRB fields have been studied using narrowband Lyα imaging (Fynbo et al. 2002, 2003; Jakobsson et al. 2005). In all cases several other galaxies at the same redshift as the GRB host were identified, but it is not clear whether the galaxy densities in these fields are higher than in blank fields, as no blank field studies have been carried out at similar redshifts. However, the density of Lyα emitters was found to be as high as in the fields around powerful radio sources that have been proposed to be forming protoclusters, which would suggest that GRBs could reside in overdense fields at $z \gtrsim 2$ (but note also that Bornancini et al. [2004] argue for a low galaxy density in GRB host galaxy environments).

To study the environment of the GRB 060505 host galaxy we searched the 2dF database for all redshift measurements within a $2^\circ \times 2^\circ$ field around the GRB 060505 host and with redshifts within $\Delta z = 0.004$ (about ± 1000 km s^{-1} at the host galaxy redshift $z_{\rm host} = 0.089$). In Figure 6 we show the field, and the result is striking. In the GRB field there is a large filamentary overdensity of galaxies with redshifts in the range 0.089–0.093. The filament extends toward the southwest from the galaxy cluster Abell 3837 at $z = 0.0896$, located at a distance of 40′ on the sky (4 Mpc in projection) from the host. This suggests that the host galaxy of GRB 060505 lies in the foreground of the galaxy cluster,

and that it may be falling into the overdense region defined by the cluster and the filament extending out from it.

6. DISCUSSION AND CONCLUSIONS

The low redshift of the host galaxy of GRB 060505 puts us in the rare fortunate situation of allowing us to study the properties in the different parts of the galaxy in a spatially resolved long-slit spectrum, including the star-forming region around the GRB site. The spatially resolved spectrum also enables us to determine for the first time the rotation curve of a GRB host galaxy, for which we find a maximum velocity of 212 km s^{-1}.

The star-forming region around the burst site is shown to be different in its properties from the rest of the galaxy. Of all the parts of the galaxy traced by the slit the burst region has the highest Hα EW, the youngest (luminosity weighted) age, and the highest luminosity-weighted star formation rate (SFR), and lies near the peak of the surface brightness distribution. Furthermore, the metallicity of the burst site is relatively low, with only 1/5 $Z_{\odot}$ according to the most recent calibrations. A low metallicity is assumed to be important for a massive star to produce a GRB (see, e.g., Woosley & Heger 2005). Also, a generally higher metallicity has been found for the environments of SNe Ic that did not produce a GRB, compared to the environment of long-duration GRBs that were accompanied by a SN Ic (Modjaz et al. 2008).

Connected to the nondetection of a SN in the light curve of GRB 060505, there have been some discussions about the classification of the burst as a long-duration GRB (Ofek et al. 2007). In addition, some concerns were put forward that the association between the GRB and the low-redshift 2dF galaxy might be due to a chance superposition (Schaefer & Xiao 2006). The clear association of the OT position with a star-forming region with a size of 400 pc, however, disfavors this possibility and strengthens the suggestion that GRB 060505 was due to the collapse of a massive star that originated in this star-forming region. Using the size of the star-forming region measured from the *HST* data of the host galaxy, and assuming that GRB 060505 was due to a merger event, Ofek et al. (2007) derive a maximum age of 10 Myr for the progenitor system assuming the lowest possible kickoff velocity from their birth site, which is consistent with the shortest time delays of a merging system (Belczynski et al. 2006).

Ofek et al. (2007) argue that the properties of the host galaxy and the location of the burst within its host provide evidence that GRB 060505 is of a different nature than other long GRBs, in particular in comparison with the sample in Fruchter et al. (2006). As shown in this paper, the properties of the host and of the birth range fall well within the range of other long GRB hosts and birth sites in the sample of Fruchter et al. (2006). In particular, similar hosts and burst locations have been found for other nearby long GRBs. The long-duration bursts GRB 980425 (Fynbo et al. 2000; Sollerman et al. 2002), GRB 990705 (Le Floc'h et al. 2002), and GRB 020819 (Jakobsson et al. 2005) were also located in the outer parts of spiral hosts. Fruchter et al. (2006) also argue that even though most GRB hosts are young, metal-poor dwarfs, long GRBs that are found in spiral galaxies would lie on the outskirts of those, preferring metal-poor, star-forming regions, which is exactly the case for GRB 060505.

Further support for the death of a massive star as the origin for this burst comes from the remarkably young age of the stellar population at the GRB site of less than 6 Myr, which is just barely consistent with even the shortest timescales needed for a binary compact object system to merge (Belczynski et al. 2006). Also, there should be no reason to expect a low metallicity for a merging system. Even though some short-duration GRBs have occurred in star-forming galaxies (e.g., Fox et al. 2005; Covino et al. 2006; Soderberg et al. 2006; Berger et al. 2007), the specific star formation of the GRB 060505 H II region is significantly larger than that inferred for these events.

Levesque & Kewley (2007) claim that the properties of the GRB region are similar to short GRB hosts in SFR and metallicity derived from emission lines. Several points in their analysis, however, are highly debatable. Instead of applying a luminosity or stellar mass–weighted specific SFR, they compare the uncorrected SFR with the one of entire short and long burst host galaxies. Furthermore, they take a "sample" of only two short GRB hosts, as their analysis requires emission lines to be able to derive metallicities for the hosts using the R_{23} parameter. This leaves out a part of the short GRB host sample, namely the ones that have been claimed to reside in early-type galaxies without ongoing star formation that are therefore inaccessible for metallicity measurements using R_{23} or similar emission-line calibrations (for a summary on the properties of early-type short GRB hosts, see Prochaska et al. 2006). In addition, one of the two bursts used in their sample is X-ray flash XRF 050416A, where evidence for a SN component at late times has been found, making this burst likely to be a collapsar event (Soderberg et al. 2007). Considering the still very small sample available for a detailed study of their properties and the large variety of short GRB hosts, a comparison between the hosts of the two types of GRBs should be taken with caution.

In our opinion, the evidence from the properties of the GRB region strongly suggests that GRB 060505 was the result of the death of a massive star that died without producing a SN. Several theoretical works have developed models to explain models of GRBs that do not produce a bright or no SN at all (Fryer et al. 2006; Tominaga et al. 2007). Our toy model of determining the nature of a GRB according to a (missing) SN connection seems to have to undergo a revision and be improved with additional information from the environment in order to draw conclusions concerning the GRB progenitor.

We thank the Paranal staff for performing the observations reported in this paper. G. Ö. thanks E. Zackrisson for integrating his model spectra over the relevant filter at the observed redshift and making these models available to us. B. M.-J. wants to thank Steven Bamford for valuable discussions about rotation curve fitting of well-resolved galaxies. The Dark Cosmology Centre is funded by the Danish National Research Foundation. K. W. thanks NWO for support under grant 639.043.302. D. M. acknowledges support from the Instrument Center for Danish Astrophysics. J. G. is supported by the Spanish research programs AYA 2004-01515 and ESP 2005-07714-C03-03.

REFERENCES

Asplund, M., Grevesse, N., Sauval, A. J., Allende Prieto, C., & Kiselman, D. 2004, A&A, 417, 751
Belczynski, K., Perna, R., Bulik, T., Kalogera, V., Ivanova, N., & Lamb, D. Q. 2006, ApJ, 648, 1110
Berger, E., et al. 2007, ApJ, 664, 1000
Bersier, D., et al. 2006, ApJ, 643, 284
Bertin, E., & Arnouts, S. 1996, A&AS, 117, 393
Blanton, M. R., et al. 2001, AJ, 121, 2358
Bornancini, C. G., Martínez, H. J., Lambas, D. G., Le Floc'h, E., Mirabel, I. F., & Minniti, D. 2004, ApJ, 614, 84
Bresolin, F., Garnett, D. R., & Kennicutt, R. C., Jr. 2004, ApJ, 615, 228
Butler, N. R. 2007, AJ, 133, 1027

Cardelli, J. A., Clayton, G. C., & Mathis, J. S. 1989, ApJ, 345, 245
Christensen, L., Hjorth, J., & Gorosabel, J. 2004, A&A, 425, 913
Colless, M., et al. 2001, MNRAS, 328, 1039
Conciatore, M. L., Capalbi, M., Vetere, L., Palmer, D., & Burrows, D. 2006, GCN Circ. 5115, http://gcn.gsfc.nasa.gov/gcn/gcn3/5115.gcn3
Covino, S., et al. 2006, A&A, 447, L5
Della Valle, M., et al. 2006, Nature, 444, 1050
Foley, S., Watson, D., Gorosabel, J., Fynbo, J. P. U., Sollerman, J., McGlynn, S., McBreen, B., & Hjorth, J. 2006, A&A, 447, 891
Fox, D. B., et al. 2005, Nature, 437, 845
Fruchter, A. S., et al. 2006, Nature, 441, 463
Fryer, C. L., Young, P. A., & Hungerford, A. L. 2006, ApJ, 650, 1028
Fukugita, M., Shimasaku, K., & Ichikawa, T. 1995, PASP, 107, 945
Fynbo, J. P. U., et al. 2000, ApJ, 542, L89
———. 2002, A&A, 388, 425
———. 2003, A&A, 406, L63
———. 2006, Nature, 444, 1047
Gal-Yam, A., et al. 2006, Nature, 444, 1053
Gehrels, N., et al. 2004, ApJ, 611, 1005
———. 2006, Nature, 444, 1044
Gonzalez Delgado, R. M., Leitherer, C., & Heckman, T. 1997, ApJ, 489, 601
Hjorth, J., et al. 2003, Nature, 423, 847
Hullinger, D., et al. 2006, GCN Circ. 5142, http://gcn.gsfc.nasa.gov/gcn/gcn3/5154.gcn3
Jakobsson, P., et al. 2005, ApJ, 629, 45
Kennicutt, R. C., Jr. 1992a, ApJS, 79, 255
———. 1992b, ApJ, 388, 310
———. 1998, ARA&A, 36, 189
Kewley, L. J., Brown, W. R., Geller, M. J., Kenyon, S. J., & Kurtz, M. J. 2007, AJ, 133, 882
Kewley, L. J., & Dopita, M. A. 2002, ApJS, 142, 35
King, A., Olsson, E., & Davies, M. B. 2007, MNRAS, 374, L34
Le Floc'h, E., Charmandaris, V., Forrest, W. J., Mirabel, I. F., Armus, L., & Devost, D. 2006, ApJ, 642, 636
Le Floc'h, E., et al. 2002, ApJ, 581, L81
———. 2003, A&A, 400, 499
Levan, A., et al. 2006, ApJ, 647, 471
Levesque, E. M., & Kewley, L. J. 2007, ApJ, 667, L121
Lilly, S. J., Carollo, C. M., & Stockton, A. N. 2003, ApJ, 597, 730
Magrini, L., Vílchez, J. M., Mampaso, A., Corradi, R. L. M., & Leisy, P. 2007, A&A, 470, 865
McBreen, S., et al. 2007, ApJ, submitted
Michałowski, M. J., et al. 2008, ApJ, 672, 817
Modjaz, M., et al. 2008, AJ, in press (astro-ph/0701246)
Ofek, E. O., Cenko, S. B., Gal-Yam, A., Peterson, B., Schmidt, B. P., Fox, D. B., & Price, P. A. 2006, GCN Circ. 5123, http://gcn.gsfc.nasa.gov/gcn/gcn3/5123.gcn3
Ofek, E. O., et al. 2007, ApJ, 662, 1129
Östlin, J., Cumming, R. J., & Bergvall, N. 2007, A&A, 461, 471
Östlin, J., Zackrisson, E., Bergvall, N., & Rönnback, J. 2003, A&A, 408, 887
Pagel, B. E. J., Edmunds, M. G., Blackwell, D. E., Chun, M. S., & Smith, G. 1979, MNRAS, 189, 95
Palmer, D., Cummings, J., Stamatikos, M., Markwardt, C., & Sakamoto, T. 2006, GCN Circ. 5076, http://gcn.gsfc.nasa.gov/gcn/gcn3/5076.gcn3
Pettini, M., & Pagel, B. E. J. 2004, MNRAS, 348, L59
Prochaska, J. X., et al. 2006, ApJ, 642, 989
Schaefer, B. E., & Xiao, L. 2006, ApJ, submitted (astro-ph/0608441)
Schlegel, D. J., Finkbeiner, D. P., & Davis, M. 1998, ApJ, 500, 525
Silva, L., Granato, G. L., Bressan, A., & Danese, L. 1998, ApJ, 509, 103
Skrutskie, M. F., et al. 2006, AJ, 131, 1163
Smartt, S. J., & Rolleston, W. R. J. 1997, ApJ, 481, L47
Soderberg, A. M., et al. 2004, ApJ, 606, 994
———. 2006, ApJ, 650, 261
———. 2007, ApJ, 661, 982
Sollerman, J., Östlin, G., Fynbo, J. P. U., Hjorth, J., Fruchter, A., & Pedersen, K. 2005, NewA, 11, 103
Sollerman, J., et al. 2002, A&A, 386, 944
Stanek, K. Z., et al. 2003, ApJ, 591, L17
Thöne, C. C., Fynbo, J. P. U., Sollerman, J., Jensen, B. L., Hjorth, J., Jakobsson, P., & Klose, S. 2006, GCN Circ. 5161, http://gcn.gsfc.nasa.gov/gcn/gcn3/5161.gcn3
Tominaga, N., Maeda, K., Umeda, H., Nomoto, K., Tanaka, M., Iwamoto, N., Suzuki, T., & Mazzali, P. A. 2007, ApJ, 657, L77
Wiersema, K., et al. 2007, A&A, 464, 529
Woosley, S. E., & Heger, A. 2005, in ASP Conf. Ser. 332, The Fate of the Most Massive Stars, ed. R. Humphreys & K. Stanek (San Francisco: ASP), 407
Yoon, S.-C., & Langer, N. 2005, A&A, 443, 643
Zackrisson, E., Bergvall, N., Olofsson, K., & Siebert, A. 2001, A&A, 375, 814
Zeh, A., Klose, S., & Hartmann, D. H. 2004, ApJ, 609, 952
Zhang, B., Zhang, B.-B., Liang, E.-W., Gehrels, N., Burrows, D. N., & Mészáros, P. 2007, ApJ, 655, L25